Journal of Applied Polymer Science

Essential Work of Fracture of Poly(ϵ-Caprolactone)/Boehmite Alumina Nanocomposites: Effect of Surface Coating

Ferenc Tuba,[1] Vincent M. Khumalo,[2] József Karger-Kocsis[1,3]

[1]Department of Polymer Engineering, Faculty of Mechanical Engineering, Budapest University of Technology and Economics, H-1111 Budapest, Muegyetem rakpart (rkp). 3, Hungary

[2]Department of Polymer Technology, Faculty of Engineering and Built Environment, Tshwane University of Technology, Pretoria 0001, Republic of South Africa

[3]MTA-BME Research Group for Composite Science and Technology, Muegyetem rkp. 3, H-1111 Budapest, Hungary

Correspondence to: J. Karger-Kocsis (E-mail: karger@pt.bme.hu)

ABSTRACT: The essential work of fracture (EWF) approach was adopted to reveal the effect of nanofillers on the toughness of poly (ϵ-caprolactone) (PCL)/boehmite alumina (BA) nanocomposites. Synthetic BA particles with different surface treatments were dispersed into the PCL matrix by extrusion melt compounding. The morphology of the composites was studied by scanning electron microscopy. Differential scanning calorimetry and wide-angle X-ray scattering were used to detect changes in the crystalline structure of PCL. Also, mode I type EWF tests, dynamic mechanical analysis, and quasi-static tensile tests were applied to study the effect of the BA nanofillers on the mechanical properties of the nanocomposites. BA was homogeneously dispersed and acted as heterogeneous crystallization nucleant and a nonreinforcing filler in PCL. The tensile modulus and yield strength slightly increased and the yield strain decreased with increasing BA content (up to 10 wt %). The effect of the BA surface treatment with octylsilane was negligible by contrast to that with alkylbenzene sulfonic acid (OS2). Like the tensile mechanical data, the essential and nonessential work of fracture parameters did not change significantly either. The improved PCL/BA adhesion in case of OS2 treatment excluded the usual EWF treatise. This was circumvented by energy partitioning between yielding and necking. The yielding-related EWF decreased, whereas the nonessential EWF increased with BA content and with better interfacial adhesion. This was attributed to the effect of matrix/filler debonding. © 2013 Wiley Periodicals, Inc. J. Appl. Polym. Sci. 129: 2950–2958, 2013

KEYWORDS: morphology; nanoparticles; nanowires and nanocrystals; polyesters; structure-property relations

Received 5 October 2012; accepted 3 January 2013; published online 15 February 2013

DOI: 10.1002/app.39004

INTRODUCTION

The essential work of fracture (EWF) approach is gaining acceptance for the determination of the plane stress toughness of highly ductile polymers in their sheet and film forms.[1–4] According to the EWF approach, stable crack growth occurring in a specimen is due to increasing work input in an inner region being filtered through the gradually increasing action of the dissipative work in the neighboring region. Thus, the total work of fracture (W_f) includes both the dissipative work in the outer plastic zone and the essential one in the inner zone (cf. Figure 1). The latter is termed the *fracture process zone* (FPZ) and the related EWF in the plane stress is a geometry-independent toughness parameter and thus represents a material property. On the other hand, the nonessential or plastic work (W_p) is a geometry-dependent parameter. The attribute plastic may suggest that in the outer fracture zone irreversible deformation takes place, but this is not always the case for polymers.

As written previously, W_f can be partitioned into two components: (1) the essential work of fracture (W_e) consumed in the inner FPZ to create new crack surfaces and (2) W_p performed in the outer plastic deformation zone (see Figure 1).

W_f, calculated from the area of the load (F)–displacement (x) curves, is determined by the following:

$$W_f = W_e + W_p \tag{1}$$

With the assumption that W_e depends on the initial cross section and W_p depends on the plastic volume [cf. Figure 1(a)], eq. (1) can be rewritten in specific terms [eqs. (2) and (3)]:

$$w_f = w_e L t + \beta w_p \cdot L^2 t \tag{2}$$

$$w_f = w_e + \beta w_p \cdot L \tag{3}$$

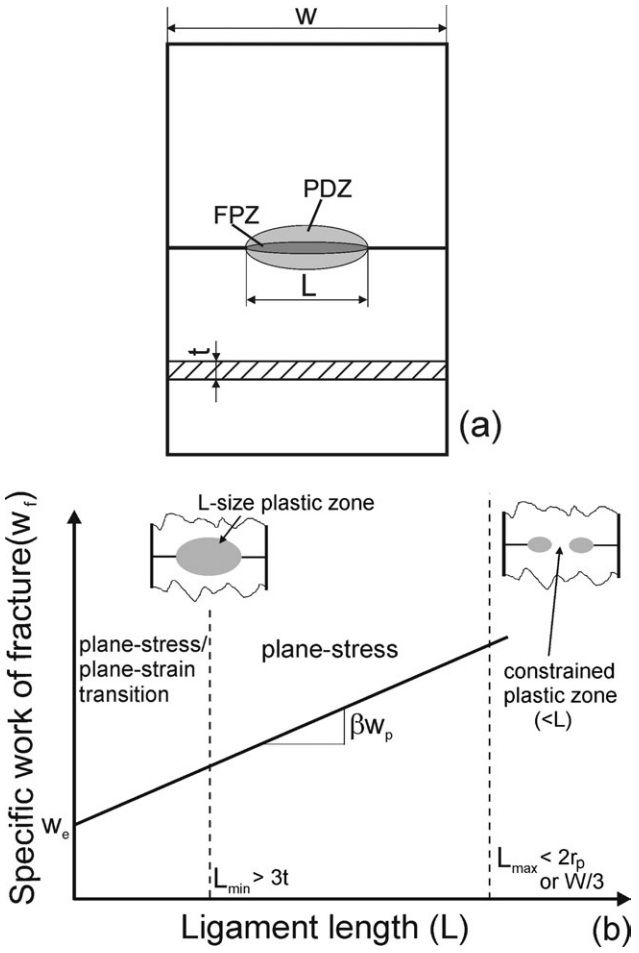

Figure 1. Schematic diagram showing the fracture zones in a DENT specimen: (a) inner FPZ and outer PDZ and (b) the data reduction method of the EWF. This figure indicates the usual criteria[3,4] for the L_{min} and L_{max} values of the valid plane-stress tests (r_p = radius of the plastic zone).

where L is the ligament length, t is the specimen thickness, and β is the shape factor related to the form of the outer plastic dissipation zone (PDZ). In the outer PDZ crazing, voiding, shear deformation, and their combination may be at work. Recall that W_e is surface-related, whereas W_p is volume-related. Equation (3) is the base of the data reduction: the specific work of fracture (w_f) data, determined on specimens with different ligaments, are plotted as a function of L. This simple mode of testing is the major reason for the popularity of the EWF approach. On the other hand, researchers often disregard whether the basic criteria of the EWF application hold or not.[4,5] These criteria[4] are the presence of quasi plane-stress conditions (taken into consideration by a valid ligament range), full ligament yielding of the specimens before crack growth (strictly taken, this is rarely fulfilled as ligament yielding and crack initiation/growth are usually superposed to one another), and self-similarity of the registered F–x curves (a minimum requirement from a practical point of view). Self-similarity means that the F–x curves at different Ls overlap by a simple linear transformation. Details on the EWF method and its application to polymers, related blends, and composites can be found in recent reviews.[1–4]

The extensive research on polymer nanocomposites has also extended to the determination of their toughness. Unfortunately, for that purpose, fracture mechanical approaches have seldom been used, albeit these are the right tools to derive toughness parameters, which are independent of the testing conditions. In addition, in many cases, it remained unclear whether the observed change in the toughness could be traced to the effects of nanofillers (e.g., dispersion characteristics, shape, specific surface data) or to nanofiller-caused fundamental changes in the morphology. Note that the latter effect is the most severe for semicrystalline thermoplastics and generates alterations in polymorphism, crystallinity (X), lamellar characteristics, tie molecule density, and so on.[5] Many researchers involved in studies devoted to the EWF testing of polymer nanocomposites have disregarded morphological changes or clearly violated the previously listed application criteria, even the less strict one, namely, the self-similarity of the F–x traces. This was pinpointed recently in a review.[4]

According to our wish to shed light on how nanofillers affect toughness, as assessed by the EWF approach, the following strategy was followed: (1) we selected polymer matrices that met the EWF requirements, (2) we chose nanofillers that could be homogeneously distributed, and (3) we used nanofillers that had a marginal impact on the morphology of the matrix. By this way, we could obtain a clearer picture on where the changes in the toughness of the polymeric nanocomposites originated from.

It has been underlined earlier that EWF-suitable matrices are amorphous copolyesters[6] and semicrystalline polypropylene copolymers.[7,8] The range of EWF-suitable semicrystalline polymers was recently extended by poly(ϵ-caprolactone) (PCL). This material fulfills all of the EWF prerequisites in its neat,[9] blend,[10] and filled (with microparticles, e.g., hydroxyapatite[11] or different types of calcium carbonate[12]) forms. The only drawback of PCL is that the melting temperature of its crystals is close to room temperature; thus, room-temperature storage (annealing) may be accompanied by morphological changes. This, however, can be circumvented by the testing of well characterized specimens with the same prehistory. The latter term means that the time interval between preparation and testing, along with the storage conditions, should be the same if the samples are to be compared.

The possible range of nanofillers having a marginal impact on the morphology in semicrystalline polymers is quite limited. Graphenes, carbon nanotubes, and organoclays usually strongly affect the crystalline structure.[5] Moreover, no homogeneous filler distribution can be achieved via conventional melt-compounding techniques. There is, however, some chance that the morphology will not be influenced and that a fine and homogeneous dispersion of nanoparticles will be achieved. Wang et al.[13] reported that TiO_2 nanoparticles, in both neat and surface-treated forms, had no significant effect on the crystalline structure. Their effect was restricted to the matrix X. The silane surface treatment of TiO_2 turned out to be beneficial with respect to the dispersion of the corresponding nanoparticles in PCL.

Boehmite alumina (BA), with a composition of AlO(OH), also seems to be a suitable nanofiller and to meet the previously

listed requirements. BA was well dispersed by melt compounding into polypropylene[14] and polyethylene,[15,16] even without any surface treatment, and had a marginal effect on the morphology of the related semicrystalline matrices. However, BA has not yet been incorporated into PCL.

Accordingly, in this study, we focused on the structure–toughness relationship in PCL/BA nanocomposites containing 5 and 10 wt % BA. To check whether the dispersion of BA was influenced by its surface treatment, BA nanoparticles with octylsilane (OS) and alkylbenzene sulfonic acid (OS2) treatments were also used. Recall that this study fit into the strategy of differentiating between the dispersion- and morphology-related effects of the nanoparticles on the toughness of the nanocomposites.

EXPERIMENTAL

Materials and Specimen Preparation

The PCL used in this study was a commercially available material (Capa 6500) procured by Perstorp UK, Ltd. (Warrington, United Kingdom) and had a nominal number-average molecular weight of 50 kDa.

As nanofiller synthetic Disperal40 boehmite of Sasol GmbH (Hamburg, Germany) was used. It had a surface area of about 100 m^2/g and a primary crystallite size of about 40 nm. BA was used in pristine and surface-treated forms. The surface treatments were done by OS (BA–OS) and C10–C13 OS2 (BA–OS2), respectively. BA was incorporated in 5 and 10 wt % concentrations, whereas the surface-modified BAs had concentrations of only 5 wt % in PCL.

The samples were prepared by melt mixing with a Berstorff corotating twin-screw extruder (ZE-40, Berstorff, Hannover, Germany) followed by granulation. The barrel temperatures from the hoper to the die were 80, 80, 85, 85, 88, 88, 90, and 90°C; the screw rotated at 60 rpm; and the melt passed through the extruder in about 80 s. Sheets with a mean thickness of 0.8 mm were produced by compression molding from the granules with a PHI press (Pasadena Hydraulics, Inc., El Monte, CA). The granules of PCL and PCL/BA were dried overnight at 60°C before compression molding. The temperature of the latter agreed with that of mixing (90°C), and the pressure was set at 2 MPa. After a 15-min holding time, the press was cooled by water.

For the tensile tests, type 1BA specimens according to ISO 527-2:1999 were cut off of the sheets. The EWF testing was performed on double-edge-notched tensile-loaded (DENT) specimens having a width (W) of 40 mm and a length of 80 mm (clamped length = 40 mm), respectively.

Dispersion of the BA Nanoparticles

The dispersion of the BA particles was studied by inspection of the surfaces of the cryofractured specimens by scanning electron microscopy (SEM). The specimens, after immersion in liquid nitrogen for 5 min, were broken by impact. SEM images were taken of the cryofractured surface of the specimens by a JEOL 6380LA scanning electron microscope (JEOL, Ltd., Tokyo, Japan) after they were coated with an Au/Pd alloy.

Melting and Crystallization Behavior of the Nanocomposites

Differential scanning calorimetry (DSC) was carried out on the samples by a TA Instruments Q2000 differential scanning calorimeter (TA Instruments, New Castle, DE). The purge gas was nitrogen (25 mL/min), and liquid nitrogen was used for cooling. The measurements were performed between −80 and 120°C with heating and cooling rates of 10°C/min. The results were evaluated according to ISO 11357-3. The X values of the samples were calculated after normalization to the nominal polymer weight fraction and with the enthalpy of fusion of the 100% crystalline polymer taken as $\Delta H_o = 142.5$ J/g.[17]

Wide-Angle X-Ray Scattering (WAXS)

To determine the possible effects of BA on the crystalline structure of PCL, WAXS measurements were performed. WAXS patterns of the polymer samples were recorded on a Phillips X-ray diffractometer (PANalytical, Almelo, The Netherlands) with a Cu Kα radiation source ($\lambda = 0.154$ nm; 45 kV and 40 mA). Data were collected in the scatter range of $2\theta = 5$–40° with a step size of 0.02°. The related X was determined by curve resolution.

Dynamic Mechanical Analysis (DMA)

DMA of the polymer sheets was performed on a TA Instruments DMA Q800 dynamic mechanical analyzer in a strain-controlled tension mode with a frequency of 1 Hz, an amplitude of 15 μm, and a force track of 120%. The properties were measured between −80 and 60°C at a heating rate of 3°C/min.

Mechanical and EWF Testing of the Nanocomposites

The tensile and fracture tests were performed under ambient conditions (24 ± 0.5°C, relative humidity = 40 ± 5%) on a Zwick Z020 universal testing machine (Zwick GmbH, Ulm, Germany). The crosshead speed was set at 10 mm/min, whereas F was recorded by a 5-kN measuring cell. The x value was calculated from the crosshead movement. For the determination of the tensile properties, five dumbbell specimens were tested for each material. For the linear regression of the EWF data, at least 20 specimens were considered. The validity of the EWF method was confirmed by the following:

- The self-similarity of F–x curves.
- A check on the ligament yielding according to method described in Ref. 18.
- As a lower ligament limit (L_{min}), which ensures quasi plane-stress conditions and steady-state crack propagation [cf. Figure 1(b)], 5 mm was found on the basis of a recommendation in our previous article.[19]
- The upper ligament limit [L_{max}, cf. Figure 1(b)] proved to be 18 mm by use of the plastic zone estimate recommended by Cotterell et al.[20] The other generally used criterion [i.e., $L < W/3$; cf. Figure 1(b)] was too conservative in this case.

All investigations were performed within a rather short time (ca. 1 week) compared to that one elapsed between the production and testing of the sheets (ca. 5 months). This guaranteed the same prehistory for the samples. Note that the alternative solution might have been rejuvenation (de-aging). This was practiced recently for a slowly crystallizing polymer, poly(lactic acid), before its EWF testing.[21]

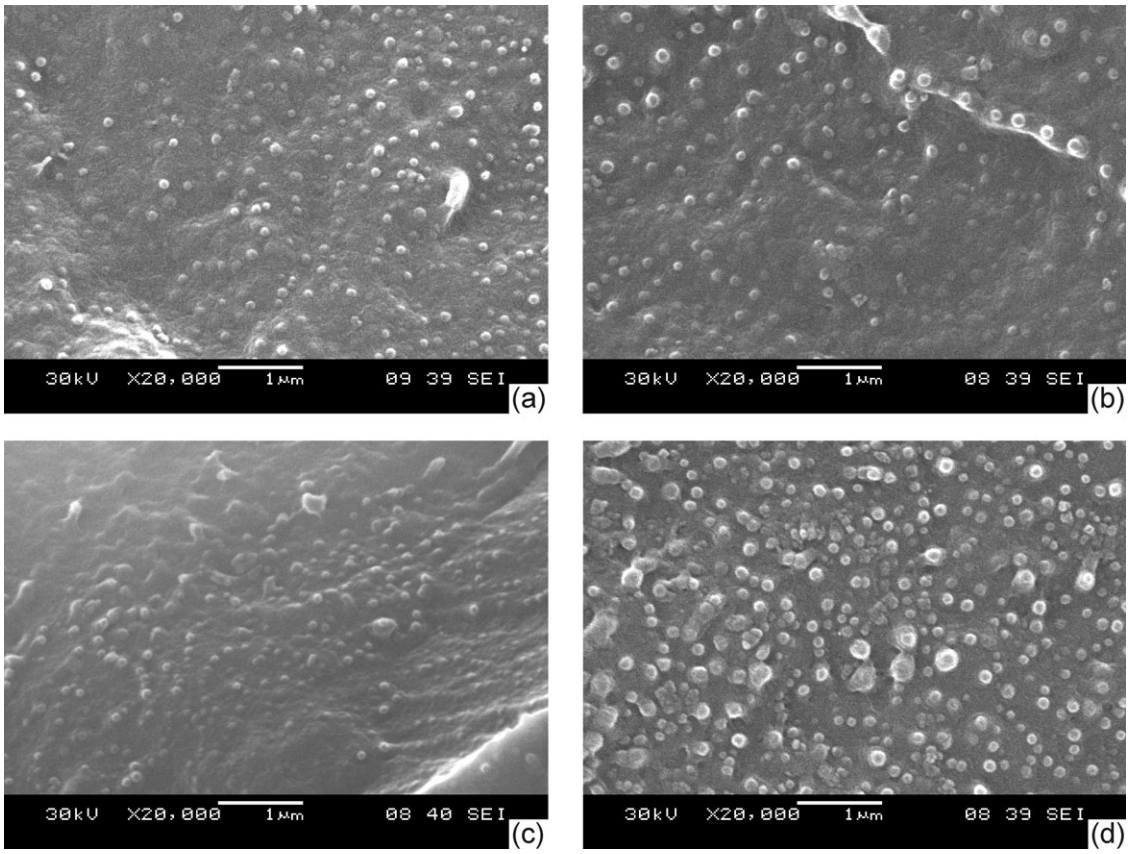

Figure 2. SEM pictures taken from the fracture surfaces of the PCL/BA nanocomposites: (a) 5 wt % BA, (b) 5 wt % BA–OS, (c) 5 wt % BA–OS2, and (d) 10 wt % BA.

RESULTS AND DISCUSSION

BA Dispersion

Figure 2 confirms by high-magnification SEM pictures that the BA was finely and homogeneously dispersed in the PCL matrix. The mean particle size was about 120 nm for the nanocomposites with 5 wt % BA; this was three times the primary crystallite size (cf. Experimental section). The mean particle size was somewhat larger, and the particle distribution was wider for the PCL/BA with a 10 wt % BA content versus that with a 5 wt % BA content. The surface treatment did not considerably affect the dispersion of the BA nanoparticles. The SEM pictures in Figure 2 confirm that BA was easily and well dispersed, in fact, in PCL. The SEM pictures served only to qualitatively assess the BA dispersion.

Melting and Crystallization of PCL/BA

Table I summarizes the DSC results derived from the first heating, cooling, and second heating cycles, respectively. The melting and related crystalline content data did not change with the type and amount of BA. On the other hand, BA worked as a nucleating agent for PCL because both the onset temperature (T_{on}) and the peak temperatures of the crystallization exotherms were shifted toward slightly higher temperatures.

The results in Table I suggest that the BA nanoparticles increased X (between 3 and 7% depending on whether the data from melting or crystallization were considered). On the other hand, the related change was less than 4% in the first heating representing the stage of the tested specimens. Moreover, the WAXS patterns (Figure 3) indicated that practically no change occurred in the crystalline fine structure of PCL due to BA incorporation. The X values deduced from the WAXS traces for the PCL/BA nanocomposites containing 0, 5 wt % BA, BA–OS, and BA–OS2 each and 10 wt % BA were 52, 57, 56, 57, and 56%, respectively. These X values agreed very well with those derived from DSC, although the latter were a bit higher.

DMA

Figure 4(a,b) shows the storage modulus (E') and loss modulus (E'') as a function of the temperature (T) for PCL and its BA nanocomposites.

BA incorporation only slightly increased the glassy modulus ($\sim$ 10%) and more markedly increased the rubbery modulus of PCL (>20%); the related data are summarized in Table II. This is characteristic for nonreinforcing (inactive) fillers, which have no strong adhesion toward the matrix and a low aspect ratio. The BA particles exhibited a low aspect ratio ($\sim$ 1) in fact, as already indicated by the SEM pictures in Figure 2. The glass-transition temperature (T_g) was not influenced significantly by the filler content or type either; this suggested that there was no significant interaction on a molecular level between the nanofiller and the PCL macromolecules. This could have been further proven by an analysis of the curve shape of T_g in the

Applied Polymer SCIENCE

Table I. Melting and Crystallization Characteristics of the PCL and PCL/BA Nanocomposites Derived from the DSC Tests

		Filler type				
		None	5 wt % BA	5 wt % BA-OS	5 wt % BA-OS2	10 wt % BA
First heating	T_{on} (°C)	57.0	58.3	59.5	57.1	60.6
	T_{mp} (°C)	61.1	65.4	67.7	65.4	66.4
	X (%)	56	60	59	59	59
Cooling	T_{on} (°C)	33.9	39.5	38.2	32.5	40.3
	T_{cp} (°C)	32.2	37.5	36.4	29.5	37.8
	X (%)	40	47	46	47	46
Second heating	T_{on} (°C)	54.3	54.1	54.4	54.0	53.6
	T_{mp} (°C)	56.6	58.7	59.0	58.4	58.5
	X (%)	47	53	50	51	50

T_{mp}, melting peak temperature; T_{cp}, crystallization peak temperature. X was normalized to the nominal amount of the PCL matrix. Parallel tests demonstrated that the scatter in X was within ±0.5%; therefore, the X data are given without decimals.

mechanical loss factor versus temperature representation. This was, however, beyond the scope of this study. Nevertheless, the DSC and DMA results confirmed that the BAs met our selection criteria with good dispersability and a marginal effect of on the morphology of the matrix.

Tensile Mechanical and EWF Results

The tensile mechanical test results are summarized in Table III. The corresponding data indicated that a 5 wt % BA incorporation increased the modulus (<17%, except for BA–OS2, where it was ~ 40%), did not affect the yield strength (σ_Y), and slightly reduced the yield strain (ϵ_Y; <7%, except for BA–OS2, where it was >40%). There was a big change in the ductility of PCL/BA–OS2 also with respect to the elongation at break. This suggests that either the molecular weight of PCL was reduced by the sulfonic acid compound, the latter improved the adhesion between PCL and BA–OS2, or both processes took place. A prominent reduction in the molecular weight should be have been associated with an enhancement in X. This was, however, not the case (cf. Table I). An increment in the tensile elastic modulus and a strong reduction in the elongation at yield and break data, being characteristic for reinforcing (active) fillers, supported the hypothesis on the improved adhesion. The big

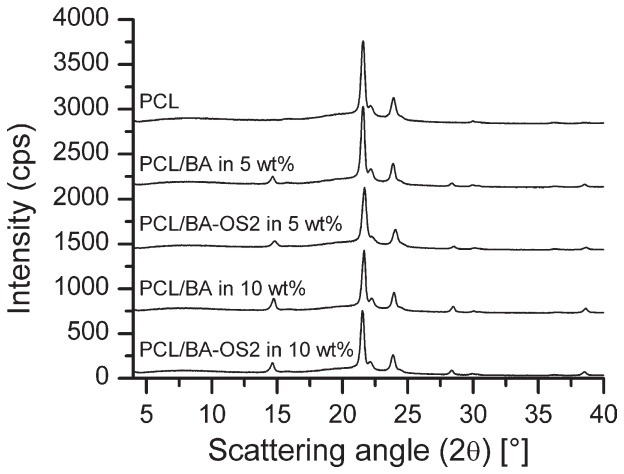

Figure 3. Wide-angle X-ray diffractograms of PCL and the PCL/BA nanocomposites. The curves were shifted vertically.

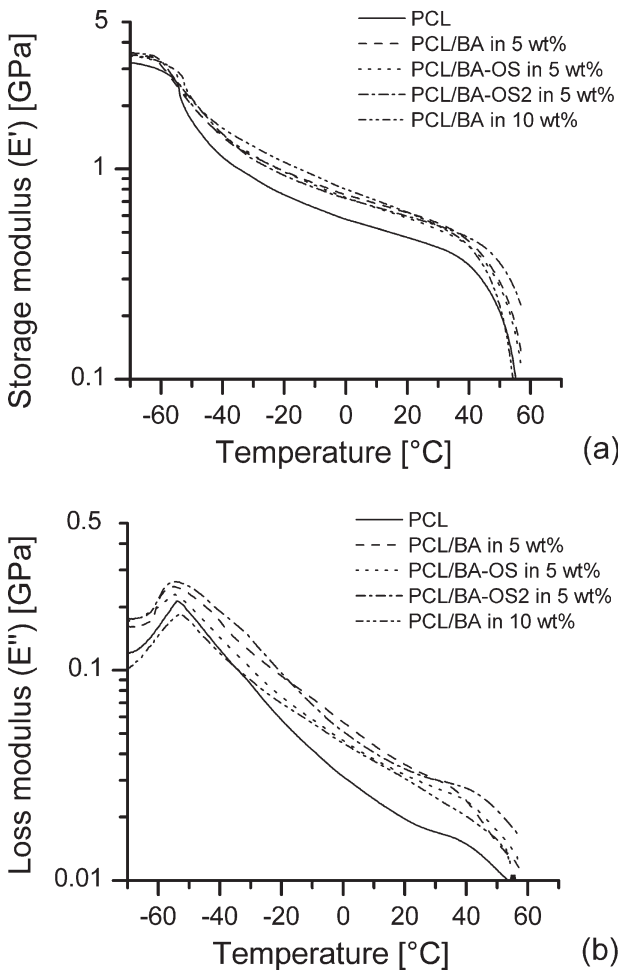

Figure 4. DMA traces in the form of (a) E' versus T and (b) E'' versus T curves for the PCL and PCL/BA nanocomposites.

Table II. Glassy and Rubbery Moduli and T_g Data for the PCL and PCL/BA Nanocomposites

Filler type	Filler amount (wt %)	E' (GPa) at $T = -70$°C	E' (GPa) at $T = 23$°C	T_g (°C)
None	0	3.20	0.46	−54.8
BA	5	3.49	0.60	−54.4
BA-OS	5	3.45	0.56	−54.7
BA-OS2	5	3.56	0.58	−54.9
BA	10	3.50	0.60	−52.7

The glassy and rubbery moduli were read at −70 and 23°C, respectively, whereas the T_g was read as the peak temperature of the E'' versus T curve.

change in the ductility was discernible in the F–x curves of the DENT specimens. Their postyield necking/tearing sections were especially affected, namely, markedly reduced.

Figure 5 shows the F–x traces of the DENT specimens as a function of their L. The neat PCL completely met the often neglected EWF prerequisite, that is, with full ligament yielding before crack formation. This was well resolved by the sudden F drops in the traces shown in Figure 5(a).[6] The self-similarity of the F–x traces is also obvious in this figure. The incorporation of BA at 5 wt % in PCL affected the ligament yielding, which was not instantaneous (i.e., droplike) any more. Nonetheless, the F–x curves remained self-similar with each other further on [cf. Figure 5(b)]. Delayed yielding and necking became even more prominent with increasing amounts of BA [cf. Figure 5(c)]; this could be explained by the higher σ_Y of the material. Such delayed yielding has been found for other semicrystalline polymers, such as syndiotactic polypropylene.[4,22] The OS surface treatment of BA had only a marginal effect on the F–x behavior compared to that of the nanocomposites with 5 wt % nanofiller contents [cf. Figure 5(b,d)]. By contrast, the F–x traces did not even meet the self-similarity criterion after the sulfonic acid treatment of BA (OS2) [cf. Figure 5(e)]. Accordingly, for the latter system, the EWF approach could hardly be adapted. On the other hand, the self-similarity still might have held for the yielding-related essential work of fracture [$w_{e,y}$; indicated by y in Figure 5(a)] of the F–x curves of PCL/BA–OS2. This could be clarified by the energy partitioning concept described in detail in Refs. 4 and 6.

For polymers with clear ligament yielding-related F drops, Karger-Kocsis[4,6] recommended the splitting of the F–x traces into yielding (y) and necking/tearing (n) related terms. This splitting is introduced also in Figure 5(a). The mathematical treatise of this energy partitioning method is given by eq. (4):

$$w_f = w_{f,y} + w_{f,n} = (w_{e,y} + \beta' w_{p,y} \cdot L) + (w_{e,n} + \beta'' w_{p,n} \cdot L) \quad (4)$$

This kind of partitioning was also followed also in this study. w_f and the specific yielding-related work of fracture ($w_{f,y}$) versus the ligament traces for the systems studied are summarized in Figure 6.

As expected, the EWF approach was blurred for the PCL/BA–OS2 system. Therefore, this nanocomposite was discarded from the EWF treatise. More exactly, only the yielding-related fracture terms were calculated, as indicated in Figure 6(e). By contrast, the w_f versus L traces for all of the other systems obeyed the linearity fairly well (cf. data in Table IV). Wong et al.[11] found similar values to ours for w_e and slightly lower values for βw_p for PCL–hydroxyapatite microcomposites. Nevertheless, it should be noted that the confidence bands of their measurements were not presented, and the deviation of their results could have been rather high because of the small specimen size selected. The latter may strongly affect the linear regression of the w_f versus L data, as stated by Pegoretti et al.[23] Additionally, the number-average molecular weights of the studied PCLs were not the same in this and Wong et al.'s[11] study, and this also influenced the w_e and βw_p parameters markedly.[24]

At the first glance, there was a rather small difference in the basic EWF parameters (i.e., w_e, βw_p) for all other systems (i.e., except that with OS2 filling), especially when we considered the related data within their 95% confidence limits. On the basis of the data in Table IV, the incorporation of BA did not affect the EWF prominently. The only exception in this respect may have been the PCL/BA 5 wt % system, for which we have no explanation at present. The EWF results suggest that the BA nanofillers (except the OS2-treated one) did not influence the molecular mobility or crystalline structure of the PCL matrix; this was in line with the DSC, DMA, and mechanical test results (cf. Tables I–III). The resistance to crack propagation, reflected by the βw_p term, decreased in the presence of the BA nanofiller. Interestingly, the amount of BA had no further effect on this term; this confirmed that BA was a nonreinforcing filler in PCL.

A deeper insight in the structure–toughness relationship was expected, however, when we collated $w_{e,y}$ and the nonessential EWF parameters, which are also incorporated into Table IV. Note that the yielding-related part of PCL with 5 wt % BA–OS2 was also analyzed by the aforementioned energy partitioning

Table III. Elastic Modulus (E), σ_Y, ϵ_Y, and Elongation at Break (ϵ_B) Values of PCL and Its BA Nanocomposites

Filler type	Filler amount (wt %)	σ_Y (MPa)	ε_Y (%)	ε_B (%)	E (MPa)
None	0	18.1 ± 0.4	15.2 ± 1.1	>400	297 ± 9
BA	5	18.4 ± 0.5	14.8 ± 1.1	>400	340 ± 17
BA-OS	5	18.3 ± 0.3	14.2 ± 1.0	>400	347 ± 10
BA-OS2	5	18.7 ± 0.9	8.4 ± 2.1	22 ± 18	418 ± 70
BA	10	20.4 ± 0.2	12.3 ± 1.2	>400	433 ± 20

Applied Polymer SCIENCE

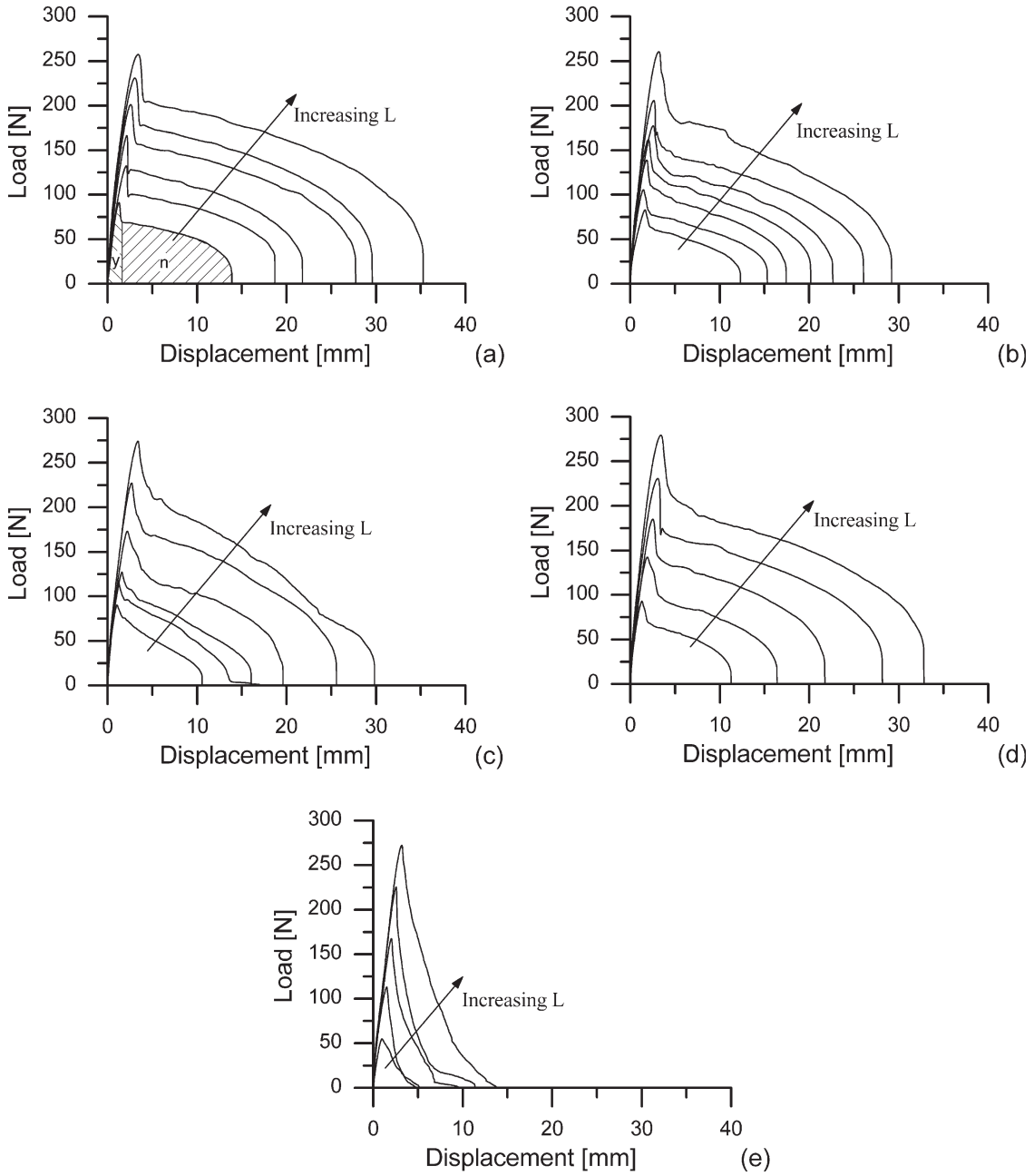

Figure 5. *F–x* traces registered for the DENT specimens of (a) PCL, (b) 5 wt % PCL/BA, (c) 10 wt % PCL/BA, (d) 5 wt % PCL/BA–OS, and (e) 5 wt % PCL/BA–OS2. With increasing *L*, both the related *F* and *x* increased.

method [cf. Figure 6(e)]. $w_{e,y}$ decreased with increasing amount of BA compared to that of PCL. The related reduction was slightly smaller for the OS-treated BA than for the neat one determined at similar regression coefficients. The reduction of $w_{e,y}$ was not surprising as nanofillers, acting as nonreinforcing particles, trigger matrix/filler debonding, which affects the yielding. Comparing the $w_{e,y}$ and ϵ_Y, as shown in Tables IV and III, respectively, we observed that they ran parallel. Recall that σ_Y did not change because of BA filling or modification (cf. Table III). The change in the $w_{e,y}$ term could be correlated with the product of ϵ_Y and σ_Y from the tensile tests. The yielding-related nonessential work of fracture term ($\beta w_{p,y}$) did not change with BA filling but reflected some changes in the surface modifications of BA. This could be attributed to debonding effects. This argument was supported by the fact that the related term of PCL–BA OS2, for which a better matrix/filler adhesion was concluded, was lower than for the other nanocomposites. Note that Table IV does not list the necking/tearing-related EWF parameters. The large scatter in these parameters did not allow us to draw any conclusions on the effects investigated. Nevertheless, their mean values could be estimated with eq. (4).

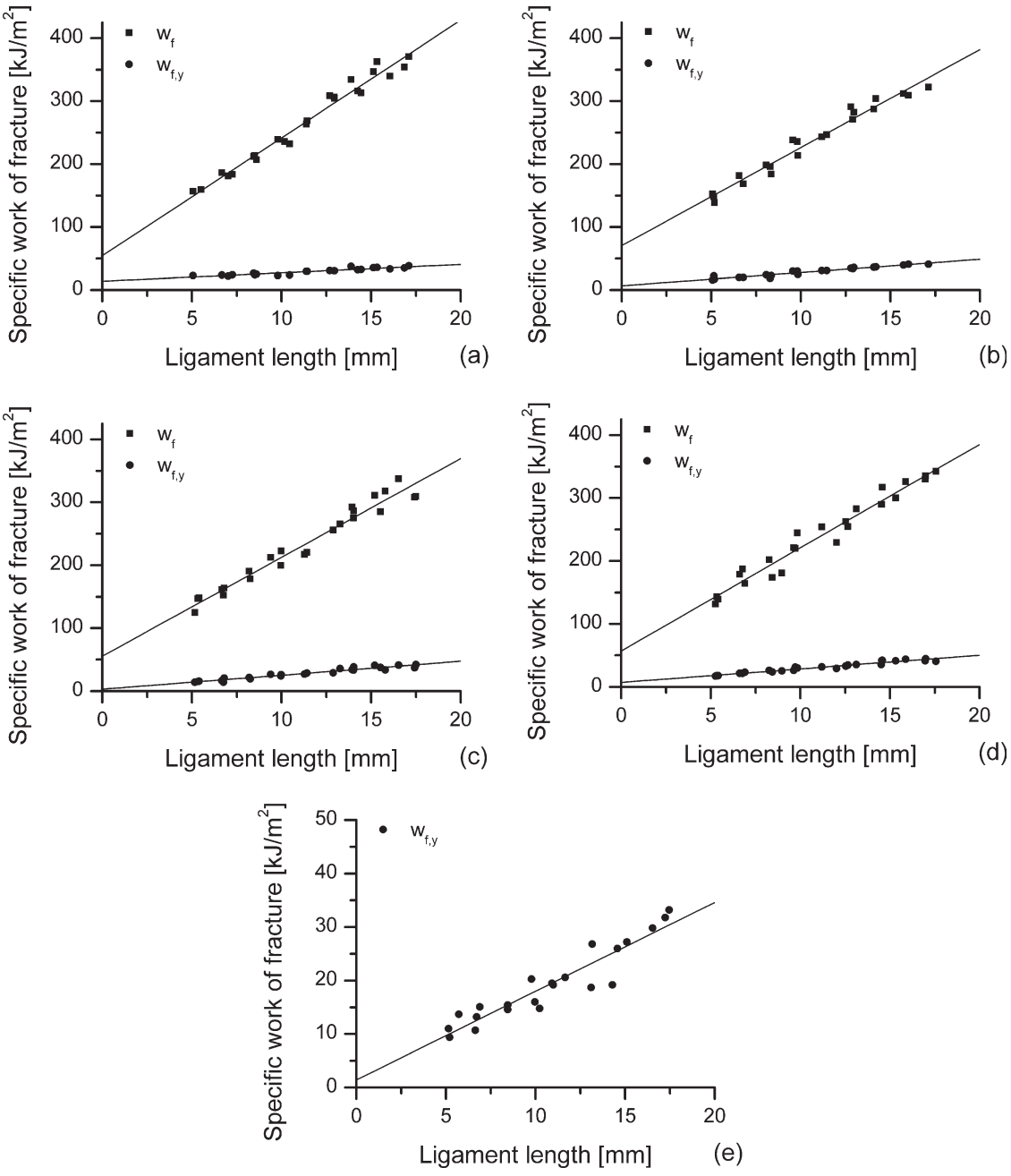

Figure 6. $w_{f,y}$ and w_y versus L traces for the PCL and its nanocomposites. Designations: (a) PCL, (b) 5 wt % PCL/BA, (c) 10 wt % PCL/BA, (d) 5 wt % PCL/BA–OS, and (e) 5 wt % PCL/BA–OS2.

Table IV. EWF Parameters (Overall and Yielding-Related) Determined for the PCL and Its BA Nanocomposites

Filler type	Filler amount (wt %)	w_e (kJ/m^2)	βw_p (MJ/m^3)	R^2 (—)	$w_{e,y}$ (kJ/m^2)	$\beta w_{p,y}$ (MJ/m^3)	R^2 (—)
None	0	54.5 ± 15.6	18.7 ± 1.3	0.98	13.9 ± 3.8	1.3 ± 0.3	0.85
BA	5	70.4 ± 15.2	15.6 ± 1.4	0.97	6.7 ± 3.2	2.1 ± 0.3	0.93
BA-OS	5	56.9 ± 17.2	16.4 ± 1.5	0.96	7.2 ± 2.7	2.2 ± 0.2	0.94
BA-OS2	5	—	—	—	1.4 ± 3.6	1.7 ± 0.4	0.88
BA	10	55.5 ± 16.6	15.7 ± 1.4	0.96	3.2 ± 3.1	2.2 ± 0.3	0.93

Data with 95% confidence limits are given.

CONCLUSIONS

In this study, the effect of boehmite (BA) nanofillers on the morphology and mechanical and fracture mechanical properties of PCL was investigated. Boehmite was selected to achieve marginal changes in the crystalline phase and thus get a clear picture of the effects caused by the nanoparticles themselves. For that purpose, PCL/BA nanocomposites containing 5 and 10 wt % BA with and without surface treatments were prepared. The BA particles were treated with OS and OS2.

The filler amount and surface treatment did not influence the filler dispersion considerably; the composites had homogeneously dispersed structures with small amounts of larger agglomerates. Slight increases in X (~3%) and the melting temperature (~4°C) were observed, and the crystallization temperatures also shifted to higher temperatures (~5°C). This was ascribed to the heterogeneous nucleating effect of the nanofillers. Neither the filler amount nor the surface treatment resulted, however, in further changes.

The DMA results indicate that there was no molecular-level interaction between the polymer and the filler; the T_g values remained unaltered. Marginal increases in rubbery and glass moduli were, however, observed. σ_Y and the elongation at break were nearly the same for the examined materials, except for the sulfonic acid treated BA-filled composite, which became more brittle than the others. The similar σ_Y, elongation at break, and E' values indicated that BA acted as a nonreinforcing filler. The elongation at yield decreased slightly, and the tensile modulus increased with increasing filler content because of the incorporation of rigid particles. Again, the surface treatment only affected the properties of the sulfonic acid treated BA composites. For this composite, better matrix/filler interfacial adhesion was observed, and this yielded a stiffer, less ductile material.

The EWF method was applicable for the composites except for the sulfonic acid treated PCL/BA composite, where the stable crack propagation and the self-similarity of F–x curves were absent. w_e also remained unaltered when we considered the 95% confidence limits, whereas the plastic work of fracture (βw_p) decreased with increasing filler content. This also underlines that a nonreinforcing filler will not improve the EWF until the crystalline morphology remains the same. On the other hand, w_p decreased with increasing amount of BA. This was accompanied by a shrinking plastic zone. The curve partitioning of the F–x curves of the EWF tests revealed that $w_{e,y}$ decreased with increasing filler content and enhanced interfacial adhesion. This observation was in line with the changes observed for the tensile yield data of the PCL/BA nanocomposites, that is, a marginal change in σ_Y and decreasing elongation at yield; these reflected that BA was a nonreinforcing filler.

ACKNOWLEDGMENTS

This work was supported by the Hungarian–Italian Bilateral program On the Toughness of Thermoplastic Nanocomposites as Studied by the Essential Work of Fracture (EWF) Approach (project ID: TÉT-10-1-2011-0218). It is also connected to the scientific programs Development of Quality-Oriented and Harmonized R + D + I Strategy and Functional Model at BME (project ID: TÁMOP-4.2.1/B-09/1/KMR-2010-0002) and Talent Care and Cultivation in the Scientific Workshops of BME (Project ID: TÁMOP-4.2.2.B-10/1-2010-0009).

REFERENCES

1. Mai, Y.-W.; Wong, S.-C.; Chen, X.-H. In Polymer Blends: Formulations and Performance;Paul, D. R.,Bucknall, C. B., Eds.; Wiley:New York, **2000**; p 17.
2. Williams, J. G.; Rink, M. *Eng. Fracture Mech.* **2007**, *74*, 1009.
3. Martinez, A. B.; Gamez-Perez, J.; Sanchez-Soto, M.; Velasco, J. I.; Santana, O. O.; Maspoch, M. L. *Eng. Failure Anal.* **2009**, *16*, 2604.
4. Bárány, T.; Czigány, T.; Karger-Kocsis, J. *Prog. Polym. Sci.* **2010**, *35*, 1257.
5. Karger-Kocsis, J. In Nano- and Micromechanics of Polymer Blends and Composites;Karger-Kocsis, J.,Fakirov, S., Eds.; Hanser:Munich, **2009**; p 425.
6. Karger-Kocsis, J. *Polym. Bull.* **1996**, *37*, 119.
7. Ferrer-Balas, D.; Maspoch, M. L.; Martinez, A. B.; Santana, O. O. *Polym. Bull.* **1999**, *42*, 101.
8. Ferrer-Balas, D.; Maspoch, M. L.; Martinez, A. B.; Ching, E.; Li, R. K. Y.; Mai, Y.-W. *Polymer* **2001**, *42*, 2665.
9. Tuba, F.; Oláh, L.; Nagy, P. *J. Mater. Sci.* **2011**, *46*, 7901.
10. Tuba, F.; Oláh, L.; Nagy, P. *Eng. Fracture Mech.* **2011**, *78*, 3123.
11. Wong, S.-C.; Baji, A.; Gent, A. N. *Compos. A* **2008**, *39*, 579.
12. Tuba, F.; Oláh, L.; Nagy, P. *J. Appl. Polym. Sci.* **2011**, *120*, 2587.
13. Wang, G.; Chen, G.; Wei, Z.; Yu, T.; Liu, L.; Wang, P.; Chang, Y.; Qi, M. *J. Appl. Polym. Sci.* **2012**, *125*, 3871.
14. Streller, R. C.; Thomann, R.; Torno, O.; Mülhaupt, R. *Macromol. Mater. Eng.* **2008**, *293*, 218.
15. Khumalo, V. M.; Karger-Kocsis, J.; Thomann, R. *Express Polym. Lett.* **2010**, *4*, 264.
16. Khumalo, V. M.; Karger-Kocsis, J.; Thomann, R. *J. Mater. Sci.* **2011**, *46*, 422.
17. Crescenzi, V.; Manzini, G.; Calzolari, G.; Borri, C. *Eur. Polym. J.* **1972**, *8*, 449.
18. Tuba, F.; Oláh, L.; Nagy, P. *Eng. Fracture Mech.*, to appear. http://dx.doi.org/10.1016/j.engfracmech.2012.12.011
19. Tuba, F.; Oláh, L.; Nagy, P. *J. Mater. Sci.* **2012**, *47*, 2228.
20. Cotterell, B.; Pardoen, T.; Atkins, A. *G. Eng. Fracture Mech.* **2005**, *72*, 827.
21. Gámez-Pérez, J.; Velazquez-Infante, J. C.; Franco-Urquiza, E.; Pages, P.; Carrasco, F.; Santana, O. O.; Maspoch, M. L. *Express Polym. Lett.* **2011**, *5*, 82.
22. Karger-Kocsis, J.; Bárány, T. *Polym. Eng. Sci.* **2002**, *42*, 1410.
23. Pegoretti, A.; Castellani, L.; Franchini, L.; Mariani, P.; Penati, A. *Eng. Fracture Mech.* **2009**, *76*, 2788.
24. Tuba, F.; Oláh, L.; Nagy, P. *Unpublished results*, **2012**.